Accepted Manuscript

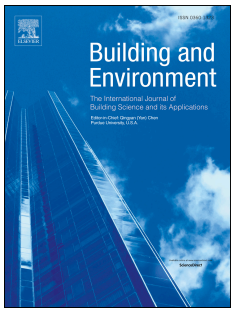

A zonal model for assessing street canyon air temperature of high-density cities

Weihui Liang, Jianxiang Huang, Phil Jones, Qun Wang, Jian Hang

PII: S0360-1323(18)30047-7

DOI: 10.1016/j.buildenv.2018.01.035

Reference: BAE 5271

To appear in: *Building and Environment*

Received Date: 24 October 2017

Revised Date: 9 January 2018

Accepted Date: 25 January 2018

Please cite this article as: Liang W, Huang J, Jones P, Wang Q, Hang J, A zonal model for assessing street canyon air temperature of high-density cities, *Building and Environment* (2018), doi: 10.1016/j.buildenv.2018.01.035.

Manuscript for ***Building and Environment***

A Zonal Model for Assessing Street Canyon Air Temperature of High-Density Cities

Weihui Liang[a,b], Jianxiang Huang[a,c*], Phil Jones[d], Qun Wang[e], Jian Hang[f]

[a]8/F Knowles Building, Department of Urban Planning and Design, the University of Hong Kong, Pokfulam Road, Hong Kong, China

[b]School of Architecture and Urban Planning, Nanjing University, Nanjing, China

[c]Shenzhen Institute of Research and Innovation, The University of Hong Kong

[d]Welsh School of Architecture, Cardiff University, King Edward VII Avenue, Cardiff CF10 3NB, UK

[e]Department of Mechanical Engineering, The University of Hong Kong, Pokfulam Road, Hong Kong Special Administrative Region

[f]School of Atmospheric Sciences, Sun Yat-Sen University, Guangzhou, P. R. China

[*]Corresponding author:

Dr. Jianxiang Huang

8/F Knowles Building, Department of Urban Planning and Design, the University of Hong Kong, Pokfulam Road, Hong Kong, China

Tel: +852 2219 4991

Fax: +852 2559 0468

Email: jxhuang@hku.hk

Abstract

The microclimate of a high-density city affects building energy consumption and thermal comfort. Despite the practical needs in building design and urban planning to predict conditions inside street canyons, literature is sparse for physics-based models that can support early stage design. Existing tools such as the Computational Fluid Dynamics (CFD) method is computationally expensive and cannot easily be coupled with other simulation models to account for solar heat gains at urban surfaces and anthropogenic heat from traffic and building HVAC systems. This paper describes a zonal model developed to assess airflow and air temperature in street canyons in high-density cities. The model takes into account 3D urban geometries, external wind, buoyancy, convective heat transfers from urban surfaces; it can simulate zonal air temperature, pressure, and airflow patterns by interactively solving mass, pressure and energy balance equations. The model was evaluated using field measurement on a 'mock-up' site consisted of movable concrete bins mimicking buildings and street canyons in high-density cities. Experiments were conducted on 3 alternative street layouts of various height-to-width aspect ratios: moderate (H/W=1), dense (H/W=2), and high-density (H/W=3). Agreements between predicted and measured air temperatures were satisfactory across 3 layouts (R2>0.964). Temperature differences between simulated and measured results were largely within 1 K. The model can provide a reliable and quick assessment of the impact of street canyons on urban heat

41 island (UHI) in high-density cities. The next step is to couple this model with building
42 energy models.

43

44 **Keywords:** Zonal Model; Urban Heat Island; Street Canyon Air Temperature;
45 Microclimate; Mock-Up Site

1. Introduction

The urban microclimate inside street canyons can have a major effect on the thermal comfort of pedestrians as well as building energy performance [1] [2]. Previous work has identified the need to assess urban microclimate in relation to the rapid growth of the urban population worldwide [3]. The growing urbanization drives the expansion of the urban area, creating more high-rise buildings, high-density cities and mega-cities [4] [5]. Building and urban design influence the urban microclimate, and human anthropogenic heat generation generally intensifies the differences between urban and rural microclimates [6]. The urban heat island (UHI) which is characterized by higher temperatures in urban areas than in rural areas is widely reported [6–8]. However, in most of the current building energy design processes, the microclimate around a building is not taken into consideration, and the energy demand is predicted using the meteorological data obtained from a suburban or rural weather station (i.e. a nearby airport) [9]. This simplification can generally lead to an overestimation of the annual heating load and underestimation of the cooling load compared to the situation with consideration of the urban microclimate around the building [10]. Thus, the studies of the urban microclimate in street canyons are significant for the optimization of urban design and building energy simulation.

Research literature on urban microclimate indicates experimental and numerical activities. The experimental approach can provide direct measurement data, showing the effects of different influencing factors such as the street layout and meteorological conditions etc. Santamouris et al. [11] measured the airflow and temperature in a deep pedestrian canyon over a week and found that there were spatial and temporal variations of the surface and air temperatures inside the canyon. Johansson [12] found that the average air temperature in the deep street canyon was 6 K lower than the shallow one and thus it was more comfortable in summer. Karra et al. [13] conducted

a field and laboratory study and found that the flow field showed a clear sensitivity to the local geometry. However, the experimental methods are expensive and only limited cases can be studied. Moreover, due to the limited number of the instruments, the measurement data is discrete in time and space. Thus, numerical methods have been developed to assess the microclimate in street canyons. The computational fluid dynamics (CFD) model is the most common numerical simulation approach which can simulate the detailed airflow and temperature distribution of the urban domain. Bruse and Fleer [14] introduced a model named ENVI-met, in which a non-hydrostatic microclimate model designed to simulate the surface-plane-air interactions in an urban environment. Chatzidimitriou and Axarli [15] simulated the effects of geometry on microclimate and comfort in the street canons by ENVI-met. Oguro et al. [16] established a wind environment database for the assessment system CASBEE-HI (Comprehensive Assessment System for Building Environmental Efficiency on Heat Island Relaxation) by CFD simulation. Yang and Li [17] used a three-dimensional urban surface energy balance model and studied the impact of urban geometry on average urban albedo and street surface temperature. The outdoor thermal environment has also been analyzed using CFD models[18,19], while the buoyancy effect of solar radiation is complex and cannot be easily accounted for in the CFD simulation of external spaces [20], although recent attempts were made coupling CFD and building energy models together [21]. Jeanjean et al. [22] analyzed the combined influence of building morphology and trees on air pollutant concentration in a neighbourhood by CFD. Wen et al. [23] performed CFD simulation and studied the flow behavior of the aeration around buildings. Many other studies used the CFD model to analyze the microclimate in the street canyons could be found [24–26]. The CFD method, despite many merits, are confronted with difficulties when applied to large districts and complex urban configurations [27] and it is computationally expansive, making it practically difficult to support building design

and urban planning practices in which reliable and quick assessment are needed at early stages.

In light of many practical limitations of CFD models, other alternatives methods were developed to assess airflow or temperature in street canyons. De La Flor and Domínguez [28] presented a numerical urban canyon model to assess the modification of climatic variables in an urban context. Musy et al. [29] proposed a zonal model to assess the indoor air temperature and flow. This method was also meaningful to the model development of outdoor microclimate simulation in street canyons. Bozonnet et al. [30] developed an empirical model to assess the airflow within the street canyon. Djedjig et al. [31] proposed a hygrothermal model of green walls and coupled it with the model of mass flows in street canyons to assess the thermal impact of green walls on buildings as well as the surrounding microclimate. Masson [32] presented an urban surface scheme for atmospheric mesoscale models. Yao et al. [20] developed a nodal network method to model the urban microclimates and validated it against field measurement data on the campus of Chongqing University. However, the vertical air temperature and flow profiles could not be predicted with this method.

This study describes the development of a zonal model to simulate the dynamic urban microclimate of street canyons in high-density cities. The horizontal and vertical temperature distributions across the simulation domain, air exchange between zones, can be simulated. Mathematical models and boundary conditions of the zonal model are described. Scale-model outdoor field experiments have been carried out and compared with the simulation results. The resulting zonal model is able to predict the time varying air temperature in street canyons quickly with acceptable accuracy, which has promising applications in the stages of urban and building design.

2. Method of the mathematic model

The basic idea of zonal modelling is to divide the street canyons into multiple zones

connected with each other. The air in each zone is assumed to be well-mixed with a uniform air temperature. The vertical division of zones is used to account for the vertical distribution of temperature within deep street canyons. Fig. 1 illustrates a typical zonal division for the outdoor environment. The height in the same level of the zones is set to be identical. Dimensions and divisions of the zones describe the building and canyon geometries and layouts of the domain. Pressure, temperature and air density in each zone of the domain follow the ideal gas law. The zonal method is based on mass and heat balances for the macroscopic volumes.

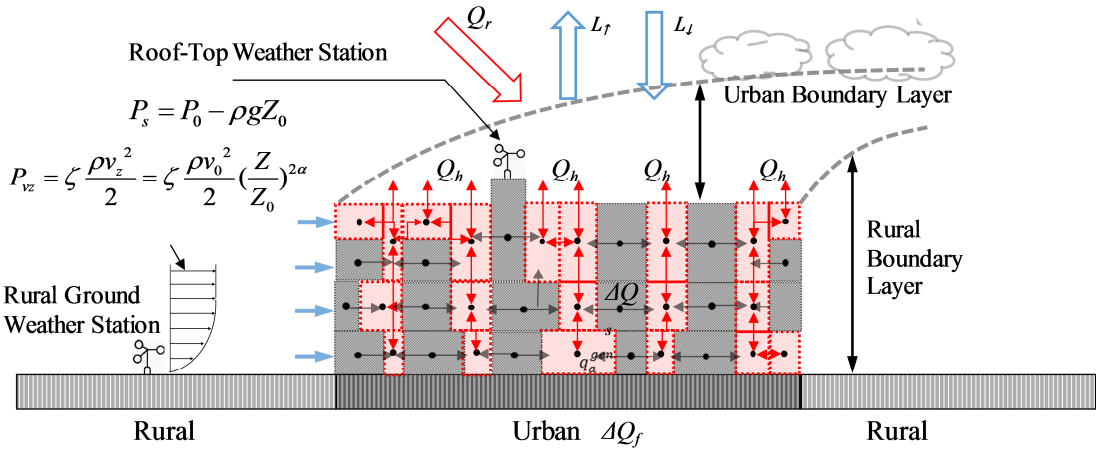

Fig. 1 Schematic depiction of the zonal urban microclimate model.

2.1 Mass and heat balances

2.1.1 Mass balance in the network

Airflow takes place across the inter-connected zones, with mass variations due to air density differences assumed negligible in an urban environment. Thus, the zonal mass balance equation can be expressed as:

$$\sum_{j=1}^{j=N} (m_{ij} - m_{ji}) = M_{si} \tag{1}$$

where m_{ij} and m_{ji} are the mass flow rate from zone i to zone j and zone j to zone i respectively (kg/s), and both are defined as "positive" variables; M_{si} is the rate of mass accumulation in zone i (kg/s), while N is the number of the zone.

2.1.2 Heat balance in the network

Heat transfer occurs between zones due to mass exchanges or between air and surfaces, i.e. building walls, roofs and the ground. The zonal heat balance equation is expressed as:

$$\rho_i V_i c_p \frac{dT_i}{dt} = \sum_{j=1}^{j=N} (m_{ji} c_p T_j - m_{ij} c_p T_i) + \sum_{k=1}^{k=M} h_k A_k (T_{surf} - T_i) + \sum_{a=1}^{a=S} Q_{si} \quad (2)$$

where the term in the left hand is the heat change of the air, the first term in the right hand represents the heat exchange due to mass flow exchange, the second term in the right hand is the convective heat flux, the third term is power of heat generation from anthropogenic source. ρ_i is the zonal air density (kg/m^3); V_i is the zonal volume (m^3); c_p is the specific heat capacity of the air (J/kg.K); T_i and T_j are the air temperature of zone i and zone j (K); h_k is the convective heat transfer coefficient between the surface and air (W/m^2.K); A_k is the area of the surface (m^2); T_{surf} is the surface temperature (K); Q_{si} is the power of heat generation from anthropogenic source within zone i (W), i.e. traffic, air conditioning (AC) units, or cooking. The surface temperature T_{surf} can be obtained by an energy balance equation on the surface or measured onsite directly.

2.2 Pressure and airflow balances

The airflow between zones is driven by pressure and density differences. Flows are calculated for 1) horizontal and 2) vertical opening accordingly. The inclined opening could be equivalent to a horizontal opening and a vertical opening with different areas

according to the projection.

2.2.1 Airflow model at horizontal opening

For horizontal openings, the hydrostatic variation of pressure between the horizontal connected two zones (ΔP_{ji}) is expressed below [22] [24] [25]:

$$\Delta P_{ji} = P_j - P_i - \frac{1}{2} g(\rho_i h_i + \rho_j h_j) \tag{3}$$

where P_j, ρ_j and h_j are the pressure, air density and overall height of the upper zone *j*. P_i. ρ_i and h_i are the pressure, air density and overall height of the bottom zone *i*. *g* is the gravitational acceleration (m/s^2).

Thus mass flow rate across the horizontal opening can be expressed as:

$$m_{ji} = \mu A \sqrt{2\rho_j \Delta P_{ji}}, \quad m_{ij} = 0, \quad \text{if } \Delta P_{ji} > 0 \tag{4}$$

$$m_{ij} = \mu A \sqrt{2\rho_i \left|\Delta P_{ji}\right|}, \quad m_{ji} = 0, \quad \text{if } \Delta P_{ji} < 0 \tag{5}$$

where μ is the discharge coefficient of the opening; *A* is the area of the opening (m^2). The discharge coefficient is depended on the opening Reynold number, wind incidence angle and direction of air flow, size and shape of the opening [35,36].

2.2.2 Airflow model at vertical opening

For vertical openings, when there is temperature difference between zones, this temperature difference will result in an air density difference, leading to a positive pressure difference at the top of the opening and a negative pressure difference at the bottom (or vice versa) [37]. Two-way airflow may occur according to the position of the neutral level. At the neutral level, the air velocity is zero, which can be determined according to the following equation.

$$Z_n = \frac{\Delta P}{(\rho_i - \rho_j)g} \tag{6}$$

where Z_n is the neutral level (m); ΔP is the pressure difference between zones (Pa). The airflow model may vary in different conditions, according to the position of the neutral level, therefore the airflow rate is categorized into the following situations.

(1) When $0 < Z_n < h$, the neutral level is within the opening. Two-way airflow occurs at the vertical opening, which can be calculated by:

$$m_{ij} = \frac{2}{3}\mu W\sqrt{2g\rho_i\left|\rho_i - \rho_j\right|}(h - Z_n)^{\frac{3}{2}} \tag{7}$$

$$m_{ji} = \frac{2}{3}\mu W\sqrt{2g\rho_j\left|\rho_i - \rho_j\right|}(Z_n)^{\frac{3}{2}} \tag{8}$$

(2) When $Z_n \le 0$, the neutral level is below the opening. The airflow is unidirectional and flows from zone *i* to zone *j*, which can be calculated by:

$$m_{ij} = \frac{2}{3}\mu W\sqrt{2g\rho_i\left|\rho_i - \rho_j\right|}\left[(h - Z_n)^{\frac{3}{2}} - (-Z_n)^{\frac{3}{2}}\right] \tag{9}$$

$$m_{ji} = 0 \tag{10}$$

(3) When $Z_n \ge h$, the neutral level is above the opening. Air flows from zone *j* to zone *i*, which can be calculated by:

$$m_{ij} = 0 \tag{11}$$

$$m_{ji} = \frac{2}{3}\mu W\sqrt{2g\rho_j\left|\rho_i - \rho_j\right|}\left[(Z_n)^{\frac{3}{2}} - (Z_n - h)^{\frac{3}{2}}\right] \tag{12}$$

where h is the overall height of the vertical opening (m); W is the width of the opening (m).

2.3 Boundary conditions

To solve the above mass and heat balance equations, the boundary conditions of the model need to be provided or calculated, which include the wind, temperature and pressure boundary conditions. There are five zones connected to the simulation domain from the adjacent surroundings, which, for example, can represent the boundary zones in the north, south, east, west directions and the upper boundary zone.

2.3.1 Wind boundary condition

The wind direction and speed will affect the wind pressure around the simulation domain. The wind velocity in the rural boundary is prescribed by a power law distribution, which is widely used in horizontal wind speed estimation[38–41]:

$$v_z = v_0 (\frac{Z}{Z_0})^{\alpha} \tag{13}$$

where v_z is the reference wind speed at height Z (m/s); v_0 is the wind speed measured at the weather station (m/s); Z_0 is the height of the weather station (m). α is an empirical constant depending on atmospheric condition, flow stabilities and surface configurations.

2.3.2 Temperature boundary condition

The air temperature of the boundary zone influences the heat transfer between the boundary and the simulation domain induced by the airflow, while surface temperatures within the domain affect the heat transfer from the surfaces to the specific zones. Thus, both air temperatures of the boundary zones and surface temperatures of the exterior building envelopes, and the exterior ground temperatures need to be provided. Air temperature of the boundaries zones, such as north, south, west, east, and upper zones of the simulated domain, are assumed to be the same as that at the local weather station. The surface temperatures of the buildings and ground

can either be calculated by a building energy and surface temperature models or measured onsite.

2.3.3 Pressure boundary condition

The static air pressure (P_s) at a given height Z can be inferred from a local weather station after adjusting for the stack effect due to gravity:

$$P_s = P_0 - \rho g(Z - Z_0) \tag{14}$$

where P_0 is the measured barometric pressure at the operational weather station (Pa) and ρ is the density of the air (kg/m^3).

The wind pressure at the boundary surfaces of the simulated domain can be calculated according to the wind profile. The main differences between east, west, south and north surrounding zones are the values of the wind pressure coefficient ζ, which varies according to the wind direction. Thus, wind pressure (P_{vz}) at the boundary surfaces can be calculated by the following equation:

$$P_{vz} = \zeta \frac{\rho v_z^{\,2}}{2} = \zeta \frac{\rho v_0^{\,2}}{2} \left(\frac{Z}{Z_0}\right)^{2\alpha} \tag{15}$$

3. Model evaluation

3.1 Experimental setup

In order to evaluate the performance of the zonal model, scale-model outdoor field experiments were conducted in a mock-up site of Sun Yat-sen university campus in suburb region of Guangzhou, China (23°4′ N, 113°23′ E). Fig. 2 shows the plan of the mock-up site. The mock-up street canyons were built with hollow concrete bins of 0.5 m × 0.5 m × 1.2 m (width × length × height) with the wall thickness of 1.5 cm. During the experiment, a total number of 620 concrete bins were aligned in parallel rows along the east-west direction. Each row has 20 concrete bins numbered 1 to 20

starting from the east to west. The space in the mock-up street canyons could be subdivide as 20 zones in accordance with the number of the concrete bins. Zone No. 12 was used as the target zone to validate the accuracy of the model. The widths of the "street canyons" were made to 1.2 m, 0.6 m, and 0.4 m, which result in aspect ratios (*H/W*) of 1, 2 and 3, respectively. The effect of the depth of the street canyon on the microclimate around the buildings can be studied. These are simplified cases compared to the actual street canyons in city. The advantages of carrying out a field experiment on the mock-up site are that it allows reliable measurement of air temperature, surface temperatures of the ground, wall and the roof, whereas in a real city these variables cannot be easily measured and it is almost impossible to account for anthropogenic heat emissions from traffic and other activities accurately. Simulations have been compared with the measurement data, which were obtained in the experiment conducted on 19−21 July 2016.

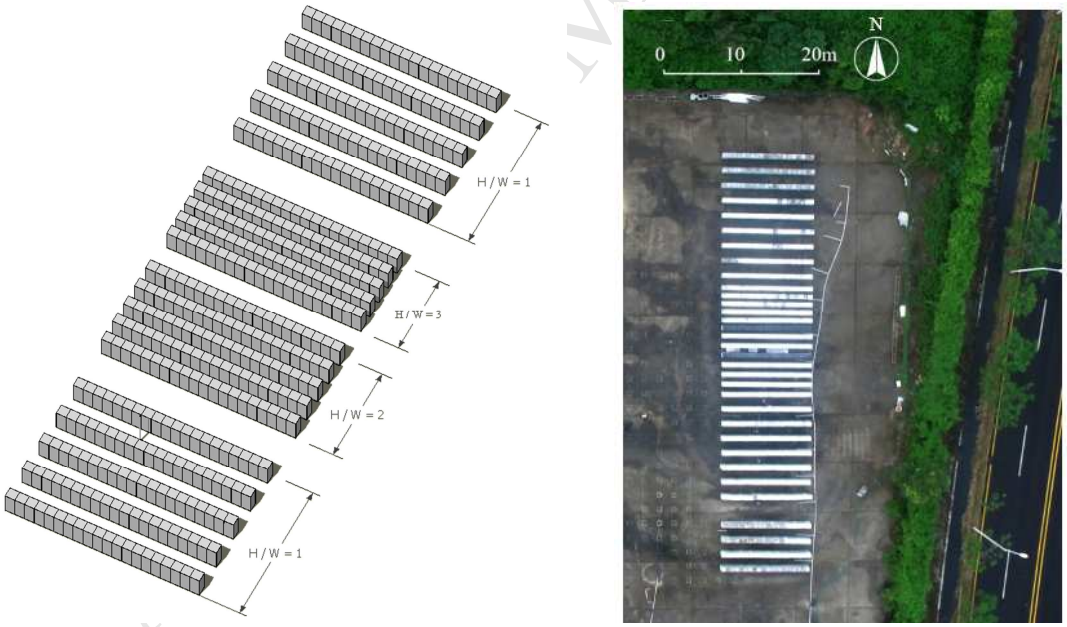

(a) (b)

(c) (d)

Fig. 2 The experiment site. (a) Schematic illustration of the plan of the mock-up street canyons with aspect ratios of moderate (*H/W*=1), dense (*H/W*=2), and high-density (*H/W*=3), (b) Aerial photo of the mock-up site taken on 18 July 2016, (c) & (d) Horizontal photos of the mock-up site taken on 18 July 2016

Measurements were conducted simultaneously and the locations of all the instruments were the same for the three different aspect ratio scenarios. Air temperatures were measured by iButton (DS 1922L) with shielding at the interval of 1 min. Two of them were placed in the center of zone No. 12 at the height of 0.1 m and 0.6 m to measure the air temperature in the mock-up street canyon. Another was placed at the height of 1.3 m to measure the air temperature above the canyons. The measurement range and error of this instrument were −40 to 85 °C and ±0.5 °C. Thermocouples were mounted on the vertical walls, the ground and roof surfaces to measure the time-varying surface temperatures. These surface temperature data were recorded continuously by Agilent 34972A data loggers at intervals of 3 seconds. Due to limited numbers of available equipment, only the surface temperatures of concrete bins No. 9−13 were measured. Thus, surface temperatures of concrete No. 12 and other concretes near it were measured in detail, which could assure the accuracy of the boundary conditions

of the target zone No. 12. Surface temperatures of concretes No. 1−8 and No. 14−20 were assumed to be the same as that of concretes No. 9 and No. 13, respectively. Several lines of thermocouples were placed alone the "wall" and "roof" surfaces to measure the temperature gradation as they were shown in Fig. 3(b)

Fig. 3. The positions of the thermocouples in the opposite "wall" and "roof" surfaces of the mock-up street canyon were the same. Five thermocouples were place evenly at the central line of the ground surface of zone No. 12 at the north-south direction. To double-check surface temperature measurement from thermocouples, an infrared camera (FLIR P635) was used to take thermal imagery of the mock-up site on a regular basis. Comparison of the surface temperature measurement results between these two methods has been illustrated in Fig. S1 of the supporting information.

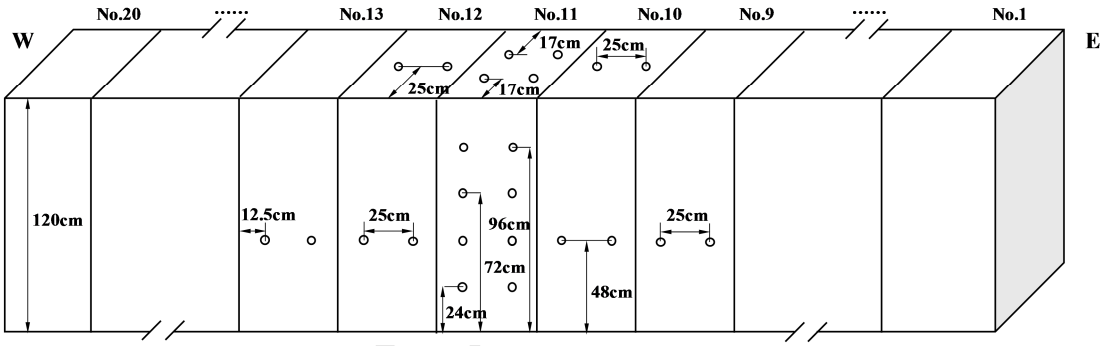

(a)

(b)

Fig. 3 Instrument layout in the mock-up street canyon. (a) Illustration of the locations of the instruments (the "○" represents the thermocouples), (b) Photo of the sensors

A weather station (RainWise PortLog) was used to measure the local air temperature, barometric pressure, solar radiation, rainfall, wind direction and speed, which could serve as the input boundary conditions for the modelling. It was located at the central of the experiment site at north-south direction. The distance between the west edge of the mock-up street canyons to the anemometer was 15 m. The monitoring time interval was set to 1 min. The sensors of the weather station were located at a height of 2.4 m above the ground. Theurer [41] concluded that for interrupted rows and row like buildings, the α value in equation 13 is recommended to be 0.36 and 0.44, respectively. The α was assumed to be 0.4 for the mock-up site in this study. Consequently, with the wind speed and height of the weather station are given, the vertical profile of the wind speed at different height could be calculated and thus the wind boundary condition could be obtained.

3.2 Measurement results

The hourly average local air temperature and barometric pressure are presented in Fig. 4(a). The air temperature ranged between 300−310 K (27−37 °C) during the measurement period. Air temperatures at 14:00, 19 and 21 July decreased noticeably due to the sudden showers at the period of 13:49−14:02, 19 July and 13:52−14:04, 21 July recorded by the local weather station. As the water absorbed by the concrete bins could not be accurately estimated when it was raining, nor the amount of moister evaporating from the surfaces after the rain, the heat exchange at the concrete surfaces due to this factor could not be well considered. Thus the effect of rain was not considered in our simulation. Consequently, the simulated temperatures supposed to be higher than the measured data at the rainy hours (13:00-14:00) and several hours after (14:00-17:00).

The hourly average wind speed and direction are shown in Fig. 4(b). Wind from the north direction corresponds to 0 ° in the figure. Recorded wind direction ranged from 76° to 250°, allowing assessment of conditions in which wind are parallel, transverse or oblique to the street canyon. The actual wind speed and direction vary over time. To simplify, hourly average wind direction and speed were used as the input boundary conditions of the model to calculate the wind pressure around the mock-up street canyons. The wind speed varied between 0.07 to 3.0 m/s and the wind direction varied between 76 to 250 ° during the experiment.

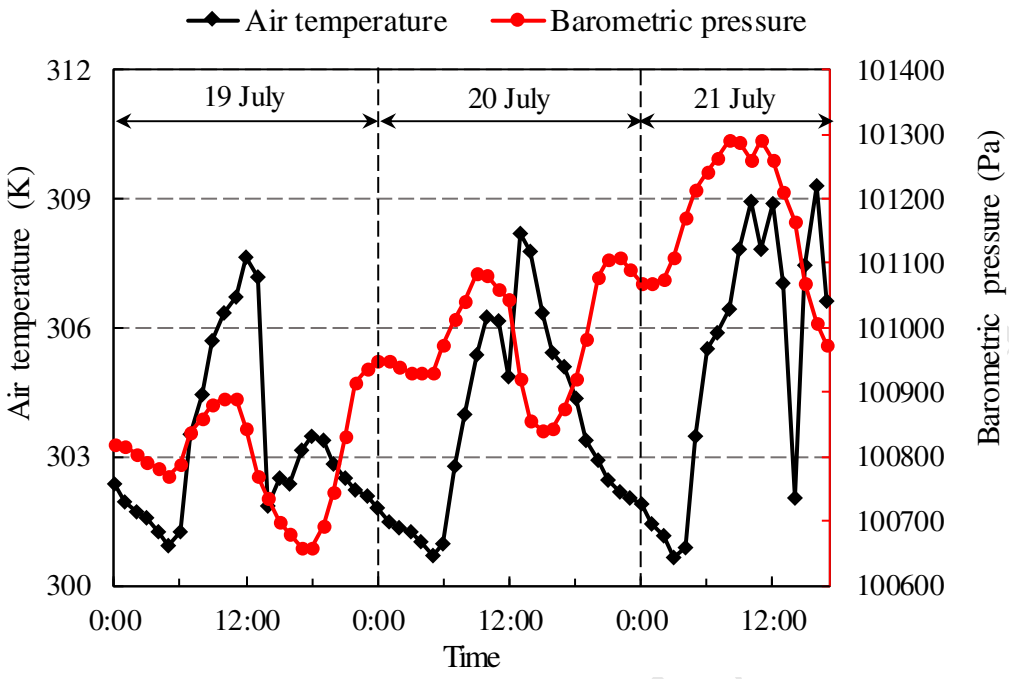

(a)

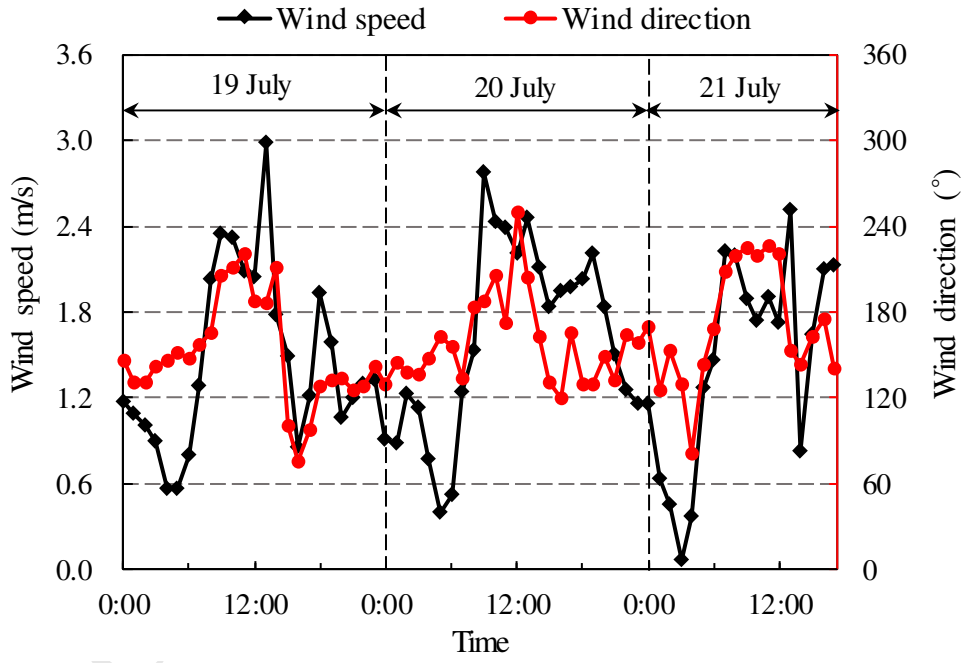

(b)

Fig. 4 Boundary conditions measured by the local weather station during the measurement. (a) Air temperature and barometric pressure, (b) Wind speed and direction (degrees from north)

Surface temperatures for different aspect ratios are presented in S2 and Fig. S2 of the Supporting Information. Air temperatures at the mock-up street canyons are presented in Fig. S3 of the Supporting Information. There were slight differences among different scenarios.

3.3 Computer simulation

The "street canyons" of the mock-up site were digitalized as inputs for the zonal model. The linear space of the "street canyon" was segmented into 20 zones of equal size, numbered 1 to 20 starting from east to west. Zone No. 21 was added on the top of the street canyon and two rows of concrete bins. The height of this upper zone was assumed to be 1.2 m and the length was 10 m. This could consider the heating or cooling effects of the roof to the upper zone of the canyons. 21 zones of the simulation domain, five boundary zones, namely the east, west, north, south and upper boundary zones were included in the simulation. Fig. 5 shows the division of the zones for the mock-up street canyon.

Generally speaking, the discharge coefficients μ in the equations for sharp-edged openings are in the range of 0.6-0.65 [35,42,43]. In our case, we have a continuous street canyon which is manually divided into zones. There are no valves nor obstructions other than the canyon walls, thus the value is supposed to be larger. A value of 1 was adopted in our simulation. Sensitivity analysis of discharge coefficients on the simulation results were also included in the Supporting Information. The air temperatures in the mock-up street canyon are not sensitive to the discharge coefficient according to the results.

By inputting the surface temperatures of each zone and the measurement data of the local weather station, together with the airflow model, heat and mass balance equations in the zones, air temperature in each zone and airflow rates between zones were simulated. The simulation results for zone No. 12 were compared with the

measured air temperature data. The calculation was executed using Python programming language. For condition in each hour, the calculation tooks less than 10 seconds to reach convergence, in which the pressure, temperature and air flow residuals are less than 0.01 Pa, 0.0001 K and 0.06 kg/s respectively. Fig. 6 shows the convergence conditions of pressure, temperature and air flow at a typical hour.

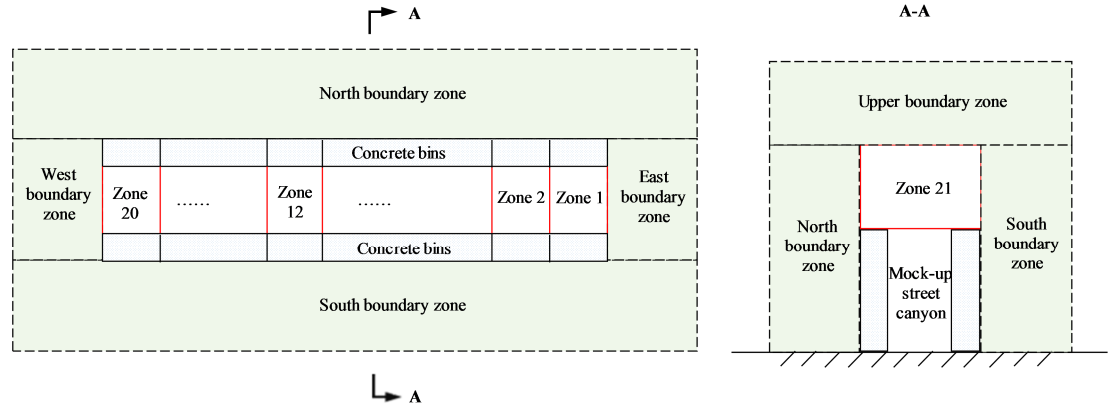

(a)

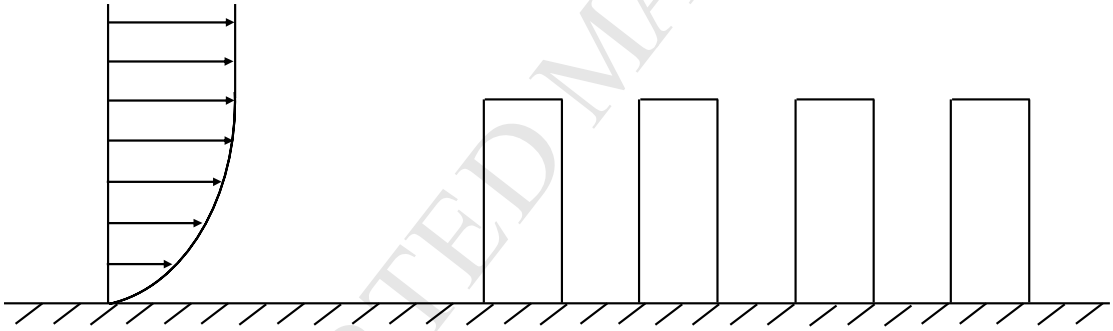

(b)

Fig. 5 (a) Division of zones for the mock-up street canyon; (b) Wind vertical profile of the study site (alpha = 0.4)

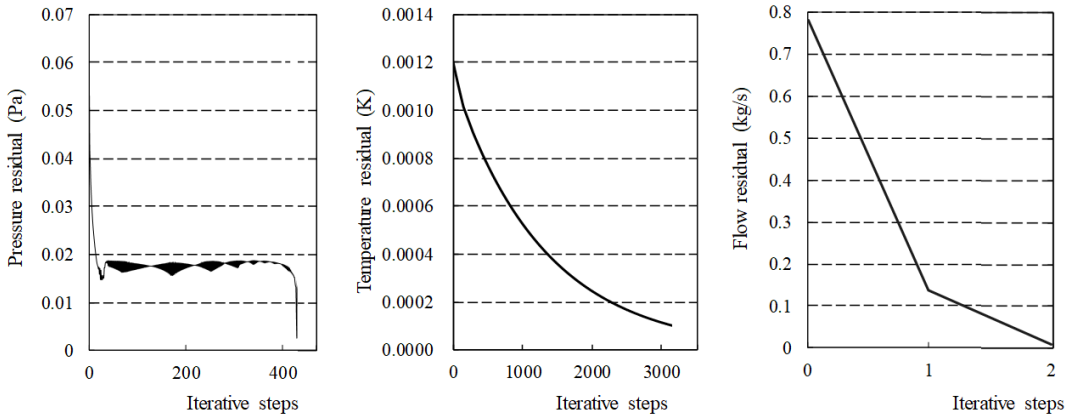

(a) (b) (c)

Fig. 6 Convergence of pressure, temperature and air flow at a typical hour. (a) Pressure residual (Pa), (b) Temperature residual (°C), (a) Airflow residual (kg/s)

382

383 **3.4 Comparison between the simulation and measurement results**

384 Fig. 7 shows the air temperature comparison between the simulated and measured
385 data for the aspect ratio of 1 (*H/W*=1). The correlation and root mean square error
386 (RMSE) value for the simulated and measured data are also presented. Simulated air
387 temperature in the mock-up street canyon showed the same variation trend as the air
388 temperature measured at the local weather station. The air in the mock-up street
389 canyon was heated by the surface of the concrete columns and can result in a higher
390 value than the air temperature at the local weather station sometimes. It could raise
391 2−6 K at noon. Correlation analysis suggested that the simulated temperatures were in
392 good agreement with the measured data. Differences between them were generally
393 within 1 K (the RMSE was 0.0025 for this case), indicating the acceptable accuracy of
394 the outdoor zonal model. Fig. 8 and Fig. 9 show the air temperature comparisons
395 between the simulated and measured data for an aspect ratio of 2 and 3, respectively.
396 Same as the case of moderate aspect ratio, good agreements between the simulated
397 and measured data were also achieved in the dense and high-density scenarios.

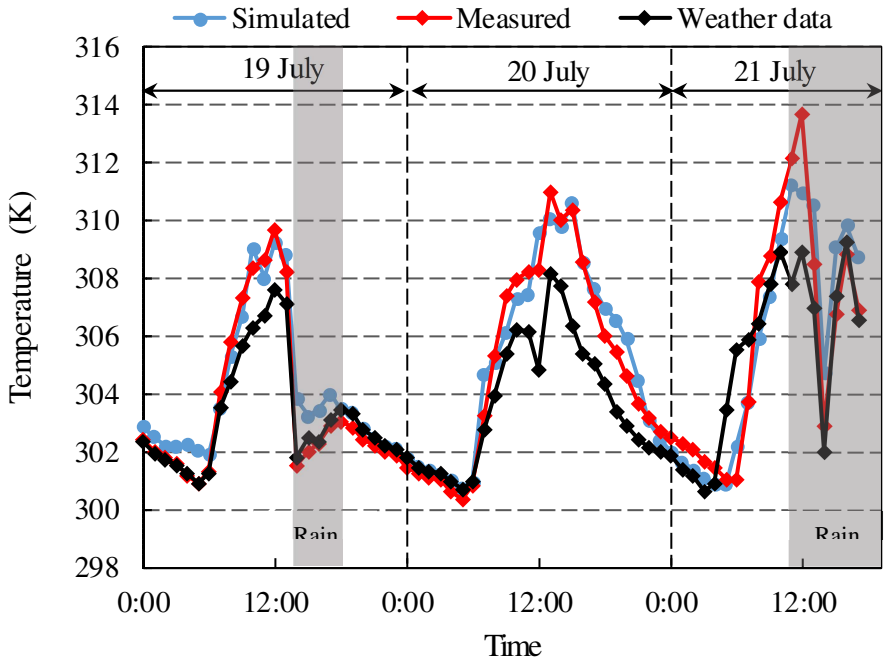

(a)

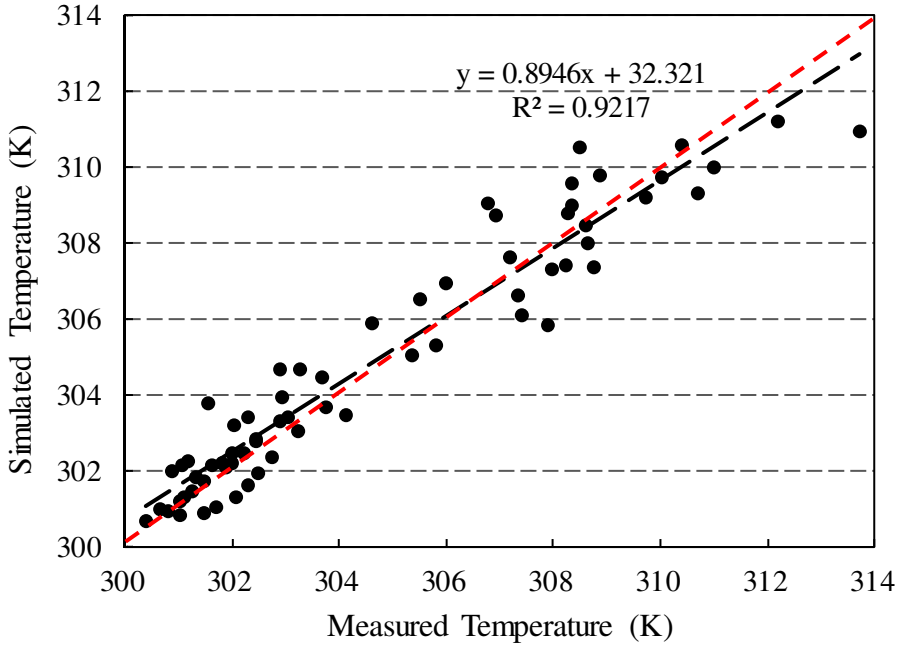

(b)

Fig. 7 Comparison of the air temperatures in the mock-up street canyon between the simulated and measured data for the moderate aspect ratio (*H*/*W*=1). (a) Comparison between the measured and simulated air temperatures, (b) Correlation analysis (RMSE=0.0035)

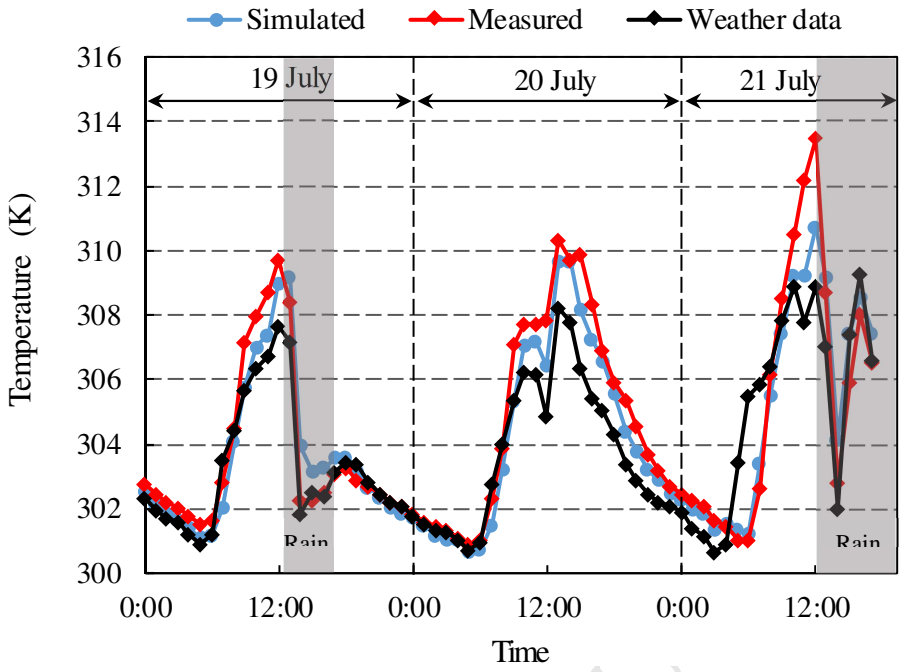

(a)

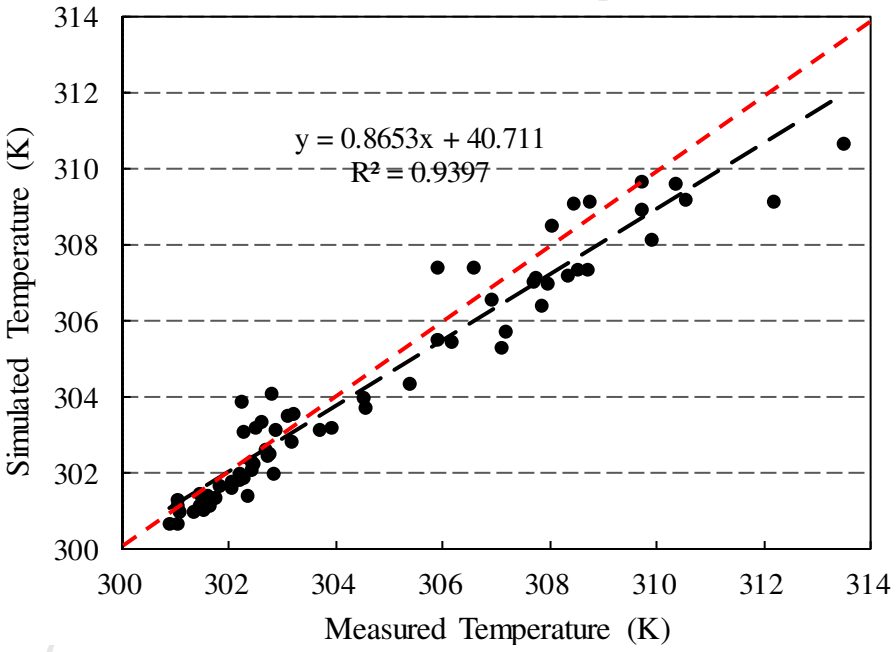

(b)

Fig. 8 Comparison of the air temperatures in the mock-up street canyon between the simulated and measured data for the dense aspect ratio (*H*/*W*=2). (a) Comparison between the measured and simulated air temperatures, (b) Correlation analysis (RMSE=0.0029)

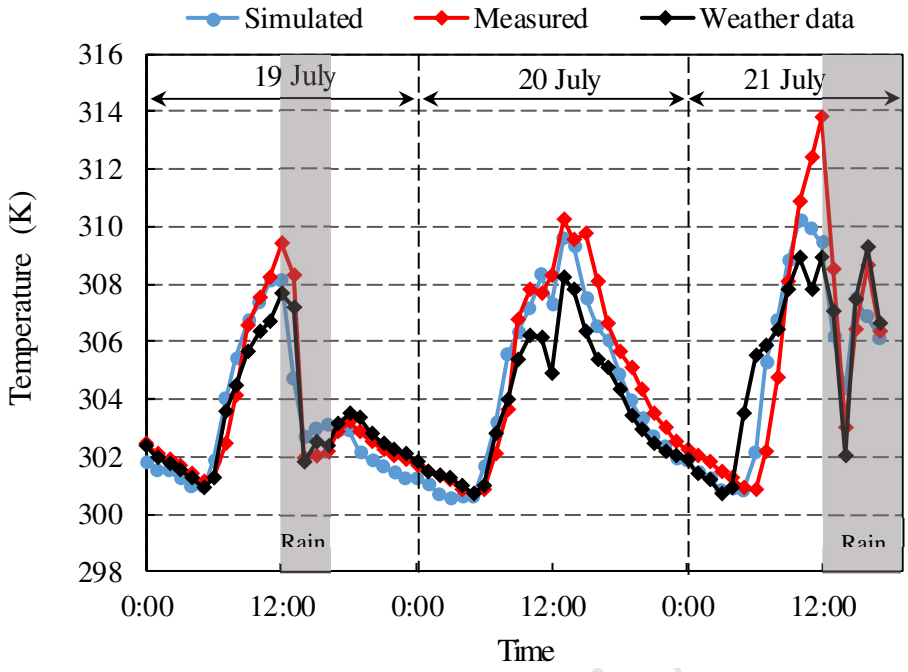

(a)

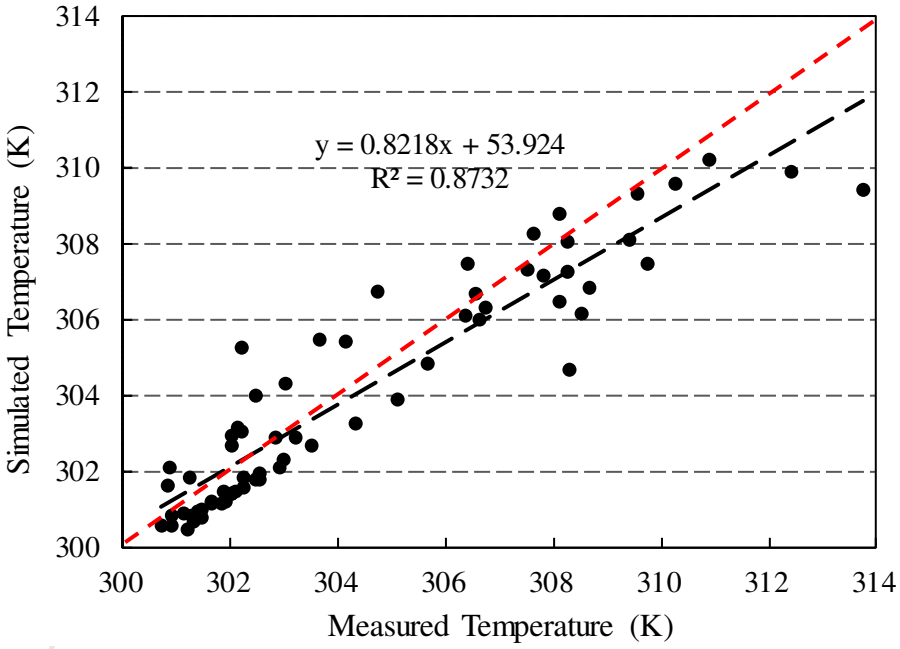

(b)

Fig. 9 Comparison of the air temperatures in the mock-up street canyon between the simulated and measured data for the high-density aspect ratio (*H*/*W*=3). (a) Comparison between the measured and simulated air temperatures, (b) Correlation analysis (RMSE=0.0041)

3.5 Strength and limitation of the zonal model

The strength of the zonal model lies in its ability to estimate urban buoyancy flow driven by solar heat gains and anthropogenic heat sources. This model is not intended to replace CFD modelling; rather, it can serve as a supplement to the existing state-of-the art methods for rapid calculation over longer time periods, for example, providing hourly values for a whole year. It is quick and it can be easily coupled with other simulation platform such as building energy models. Results can be convenient illustrated for practical applications. The airflow pattern as well as temperature profile of the street canyon with aspect ratio of 3 at 13:00 Jul.20 are presented in Fig. 10. The air from the boundary zone came from the west direction, heated by the ground and vertical surfaces of the mock-up street canyon. Air temperature in the canyon increased from the west to east consequently.

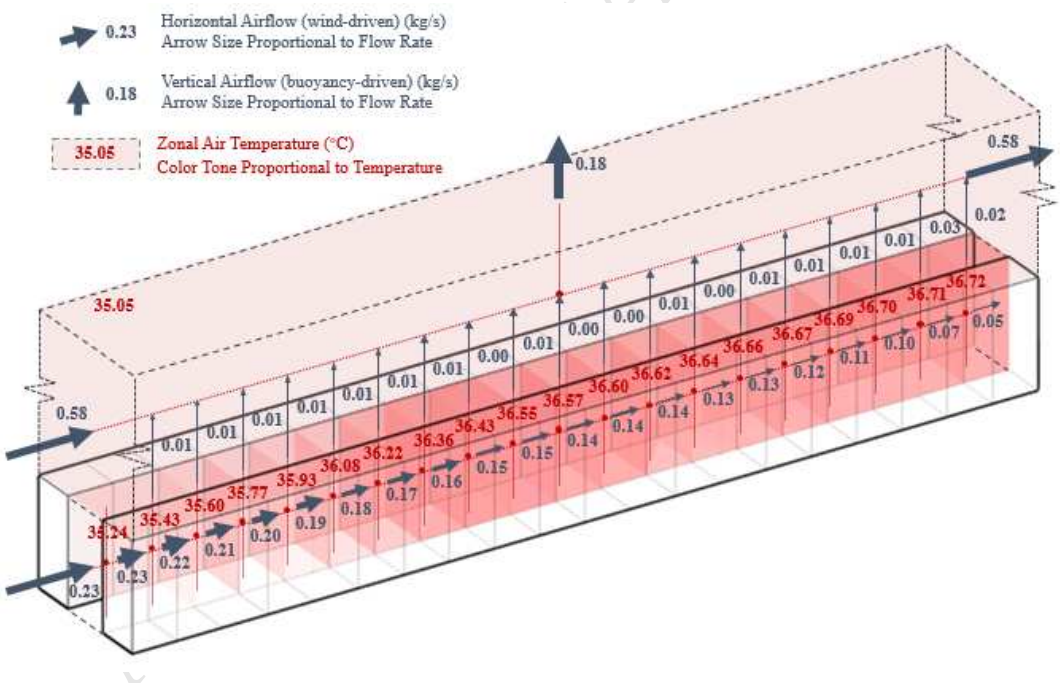

Fig. 10 Visualization of predicted zonal air temperature and inter-zonal airflow rate in the mock-up street canyon with aspect ratio of 3 at 13:00 Jul.20, 2016

The limitation of the zonal model lies in its lack of turbulence model. In order to examine the impact of turbulence characteristics on canyon temperature, we conducted CFD simulation of the study site using ANSYS Fluent as well as tracer-gas experiment. Results show that the zonal model prediction has limitations in the presence of strong turbulence introduced by perpendicular wind in medium density urban configuration (H/W=1). This effect is more prominent with wind perpendicular to street canyon consisted of uniform height buildings, where prediction from the zonal model can be over 1 °C higher than measurement data under our study site conditions. However, the impact of turbulence is subdued in high-density conditions (aspect ratio H/W=3) or under parallel wind, in which predictions from the zonal model agree very closely with those from the CFD model and measurement data (within 0.3 °C). Detailed analysis and discussions are featured in the Supporting Information.

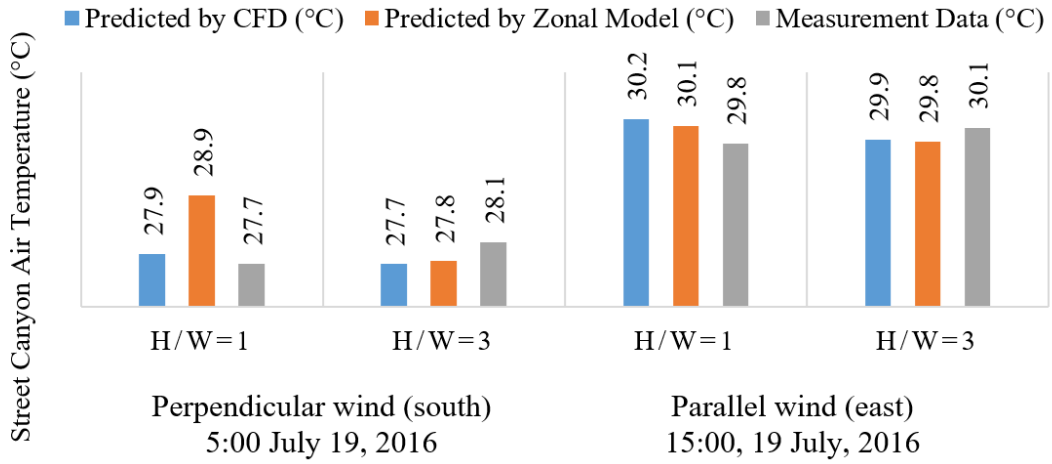

Time	5:00, 19 July		15:00, 19 July	
Dominant wind direction	Perpendicular wind (south)		Parallel wind (east)	
Aspect ratio	H/W=1	H/W=3	H/W=1	H/W=3
CFD predicted temperature (°C)	27.89	27.72	30.21	29.85
Zonal model predicted temperature (°C)	28.90	27.77	30.08	29.82
Measured air temperature (°C)	27.73	28.09	29.78	30.05

Fig. 11 Predicted street canyon air temperature by CFD and zonal model in

comparison with measurement data.

4. Conclusion

This paper described a zonal model developed to simulate urban microclimate conditions in street canyons. Outdoor field measurements have been carried out for mock-up street canyons constructed from concrete bins including zones with three different aspect ratios (*H/W*=1, 2, 3) on a campus environment to evaluate the model performance. Air temperature in the mock-up street canyons could increase up to 6 K above the ambient conditions at the noon, suggesting the necessity to consider the urban microclimate around the buildings. Predicted air temperatures for the mock-up street canyons showed satisfactory agreement with measurement data (within 1 K) for all three aspect ratio cases. The zonal model can predict in-situ air temperature in high-density cities, and, due to its fast computing speed, can potentially support early stage design. The next step is to couple the zonal model with building energy models to simulate annual hourly solar radiation, surface energy balance, and anthropogenic heat sources for a cluster of buildings in urban context.

Acknowledgements

The study is supported by the 33rd Round PDF/RAP Scheme, the Seed Fund for Basic Research (#201509159015) from the University of Hong Kong, the National Natural Science Foundation of China (No 51478486) and the National Science Fund for Distinguished Young Scholars (No 41425020). We appreciate the valuable insight and feedback from Prof. Yuguo Li of the Department of Mechanical Engineering at the University of Hong Kong.

References

[1] Y. Zhu, J. Liu, A. Hagishima, J. Tanimoto, Y. Yao, Z. Ma, Evaluation of coupled outdoor and indoor thermal comfort environment and anthropogenic heat, Build. Environ. 42 (2007) 1018–1025.

[2] J. Bouyer, C. Inard, M. Musy, Microclimatic coupling as a solution to improve building energy simulation in an urban context, Energy Build. 43 (2011) 1549–1559.

[3] L. Kamal-chaoui, A. Robert, J.E.L.C. Q, Competitive cities and climate change, Cities. (2009) 172.

[4] A.G. Aguilár, P.M. Ward, Globalization, regional development, and mega-city expansion in Latin America: Analyzing Mexico city's peri-urban hinterland, Cities. 20 (2003) 3–21.

[5] E. Ng, Towards planning and practical understanding of the need for meteorological and climatic information in the design of high-density cities: A case-based study of Hong Kong, Int. J. Climatol. 32 (2012) 582–598.

[6] A.M. Rizwan, L.Y.C. Dennis, C. Liu, A review on the generation, determination and mitigation of Urban Heat Island, J. Environ. Sci. 20 (2008) 120–128.

[7] T.R. Oke, City Size and the Urban Heat Island, Atmos. Environ. 7 (1973) 769–779.

[8] J. Yang, Z.H. Wang, K.E. Kaloush, H. Dylla, Effect of pavement thermal properties on mitigating urban heat islands: A multi-scale modeling case study in Phoenix, Build. Environ. 108 (2016) 110–121.

[9] A. Gros, E. Bozonnet, C. Inard, Cool materials impact at district scale - Coupling building energy and microclimate models, Sustain. Cities Soc. 13 (2014) 254–266.

[10] E. Erell, T. Williamson, Comments on the correct specification of the analytical CTTC model for predicting the urban canopy layer temperature, Energy Build. 38 (2006) 1015–1021.

[11] M. Santamouris, N. Papanikolaou, I. Koronakis, I. Livada, D. Asimakopoulos, Thermal and air flow characteristics in a deep pedestrian canyon under hot weather conditions, Atmos. Environ. 33 (1999) 4503–4521.

[12] E. Johansson, Influence of urban geometry on outdoor thermal comfort in a hot dry climate: A study in Fez, Morocco, Build. Environ. 41 (2006) 1326–1338.

[13] S. Karra, L. Malki-Epshtein, M.K.A. Neophytou, Air flow and pollution in a

real, heterogeneous urban street canyon: A field and laboratory study, Atmos. Environ. 165 (2017) 370–384.

[14] M. Bruse, H. Fleer, Simulating surface-plant-air interactions inside urban environments with a three dimensional numerical model, Environ. Model. Softw. 13 (1998) 373–384.

[15] A. Chatzidimitriou, K. Axarli, Street canyon geometry effects on microclimate and comfort; A case study in Thessaloniki, Procedia Environ. Sci. 38 (2017) 643–650.

[16] M. Oguro, Y. Morikawa, S. Murakami, K. Matsunawa, A. Mochida, H. Hayashi, Development of a wind environment database in Tokyo for a comprehensive assessment system for heat island relaxation measures, J. Wind Eng. Ind. Aerodyn. 96 (2008) 1591–1602.

[17] X. Yang, Y. Li, The impact of building density and building height heterogeneity on average urban albedo and street surface temperature, Build. Environ. 90 (2015) 146–156.

[18] X. Li, Z. Yu, B. Zhao, Y. Li, Numerical analysis of outdoor thermal environment around buildings, Build. Environ. 40 (2005) 853–866.

[19] B. Lin, X. Li, Y. Zhu, Y. Qin, Numerical simulation studies of the different vegetation patterns' effects on outdoor pedestrian thermal comfort, J. Wind Eng. Ind. Aerodyn. 96 (2008) 1707–1718.

[20] R. Yao, Q. Luo, B. Li, A simplified mathematical model for urban microclimate simulation, Build. Environ. 46 (2011) 253–265.

[21] S. Gracik, M. Heidarinejad, J. Liu, J. Srebric, Effect of urban neighborhoods on the performance of building cooling systems, Build. Environ. 90 (2015) 15–29.

[22] A. Jeanjean, R. Buccolieri, J. Eddy, P. Monks, R. Leigh, Air quality affected by trees in real street canyons: The case of Marylebone neighbourhood in central London, Urban For. Urban Green. 22 (2017) 41–53.

[23] C.Y. Wen, Y.H. Juan, A.S. Yang, Enhancement of city breathability with half open spaces in ideal urban street canyons, Build. Environ. 112 (2017) 322–336.

[24] Z.T. Ai, C.M. Mak, CFD simulation of flow in a long street canyon under a perpendicular wind direction: Evaluation of three computational settings, Build. Environ. 114 (2017) 293–306.

[25] X. Jin, L. Yang, X. Du, Y. Yang, Transport characteristics of PM2.5inside urban street canyons:The effects of trees and vehicles, Build. Simul. 10 (2017) 1–14.

[26] M. Moradpour, H. Afshin, B. Farhanieh, A numerical study of reactive

pollutant dispersion in street canyons with green roofs, Build. Simul. (2017).

[27] L. Yang, Y. Li, Thermal conditions and ventilation in an ideal city model of Hong Kong, in: Energy Build., 2011: pp. 1139–1148.

[28] F.S. De La Flor, S.A. Domínguez, Modelling microclimate in urban environments and assessing its influence on the performance of surrounding buildings, in: Energy Build., 2004: pp. 403–413.

[29] M. Musy, E. Wurtz, F. Winkelmann, F. Allard, Generation of a zonal model to simulate natural convection in a room with a radiative/convective heater, Build. Environ. 36 (2001) 589–596.

[30] E. Bozonnet, R. Belarbi, F. Allard, Modelling air flows around buildings in urban environment, Int. Work. Energy Perform. Environ. Qual. Build. (2006) 1–6.

[31] R. Djedjig, E. Bozonnet, R. Belarbi, Modeling green wall interactions with street canyons for building energy simulation in urban context, Urban Clim. 16 (2016) 75–85.

[32] V. Masson, A physically-based scheme for the urban energy budget in atmospheric models, Boundary-Layer Meteorol. 94 (2000) 357–397.

[33] C. Inard, H. Bouia, P. Dalicieux, Prediction of air temperature distribution in buildings with a zonal model, Energy Build. 24 (1996) 125–132.

[34] A.C. Megri, F. Haghighat, Zonal Modeling for Simulating Indoor Environment of Buildings: Review, Recent Developments, and Applications, HVAC&R Res. 13 (2007) 887–905.

[35] C.R. Chu, Y.H. Chiu, Y.J. Chen, Y.W. Wang, C.P. Chou, Turbulence effects on the discharge coefficient and mean flow rate of wind-driven cross-ventilation, Build. Environ. 44 (2009) 2064–2072.

[36] Y. Li, A. Delsante, J. Symons, Prediction of natural ventilation in buildings with large openings, Build. Environ. 35 (2000) 191–206.

[37] S.W. Dols, G.N. Walton, CONTAMW 2 . 0 User Manual, U.S. Dep. Commer. (2002).

[38] C. Chang, R.N. Meroney, Numerical and physical modeling of bluff body flow and dispersion in urban street canyons, J. Wind Eng. Ind. Aerodyn. (2001) 1–8.

[39] J.S. Irwin, A theoretical variation of the wind profile power-law exponent as a function of surface roughness and stability, Atmos. Environ. 13 (1979) 191–194.

[40] A. Albani, M.Z. Ibrahim, Wind energy potential and power law indexes

583 assessment for selected near-coastal sites in Malaysia, Energies. 10 (2017) 1–
584 21.

585 [41] W. Theurer, W. Baechlin, E.J. Plate, Model study of the development of
586 boundary layers above urban areas, J. Wind Eng. Ind. Aerodyn. 41 (1992) 437–
587 448.

588 [42] P.A. Favarolo, H. Manz, Temperature-driven single-sided ventilation through a
589 large rectangular opening, Build. Environ. 40 (2005) 689–699.

590 [43] D. Etheridge, Natural ventilation of buildings: theory, measurement and design,
591 2011.

Figure captions

Fig. 1 Schematic depiction of the zonal urban microclimate model. (The solid blocks describe the buildings)

Fig. 2 The experiment site. (a) Schematic illustration of the plan of the mock-up street canyons with aspect ratios of moderate (*H/W*=1), dense (*H/W*=2), and high-density (*H/W*=3), (b) Aerial photo of the mock-up site taken on 18 July 2016, (c) Horizontal photos of the mock-up site taken on 18 July 2016

Fig. 3 Instrument layout in the mock-up street canyon. (a) Illustration of the locations of the instruments (the "○" represents the thermocouples), (b) Photo of the sensors

Fig. 4 Boundary conditions measured by the local weather station during the measurement. (a) Air temperature and barometric pressure, (b) Wind speed and direction

Fig. 5 Division of zones for the mock-up street canyon

Fig. 12 Convergence of pressure, temperature and air flow at a typical hour. (a) Pressure residual, (b) Temperature residual, (a) Airflow residual

Fig. 7 Comparison of the air temperatures in the mock-up street canyon between the simulated and measured data for the moderate aspect ratio (*H/W*=1). (a) Comparison between the measured and simulated air temperatures, (b) Correlation analysis (RMSE=0.0025)

Fig. 8 Comparison of the air temperatures in the mock-up street canyon between the simulated and measured data for the dense aspect ratio (*H/W*=2). (a) Comparison between the measured and simulated air temperatures, (b) Correlation analysis (RMSE=0.0029)

Fig. 9 Comparison of the air temperatures in the mock-up street canyon between the

simulated and measured data for the high-density aspect ratio (*H/W*=3). (a) Comparison between the measured and simulated air temperatures, (b) Correlation analysis (RMSE=0.0041)

Fig. 10 Visualization of predicted zonal air temperature and inter-zonal airflow rate in the mock-up street canyon with aspect ratio of 3 at 13:00 Jul.20, 2016

Research Highlights

- Developed a zonal model to assess street canyon air temperature of high-density cities
- The model was evaluated in field measurement on a mock-up site with 3 aspect ratios
- Good agreements between predicted and measured air temperatures were observed(<1 K)
- Peak warming between 2-6 K above the ambient air temperature were observed in mockup street canyons